

Control of Dephasing and Phonon Emission in Coupled Quantum Dots

S. Debold¹, T. Brandes², and B. Kramer¹

¹ *University of Hamburg, 1. Inst. Theor. Physik, Jungiusstr. 9, 20355 Hamburg, Germany and*

² *Department of Physics, University of Manchester Institute of Science and Technology (UMIST), P.O. Box 88, Manchester M60 1QD, United Kingdom*

(Dated: November 1, 2018)

We predict that phonon subband quantization can be detected in the non-linear electron current through double quantum dot qubits embedded into nano-size semiconductor slabs, acting as phonon cavities. For particular values of the dot level splitting Δ , piezo-electric or deformation potential scattering is either drastically reduced as compared to the bulk case, or strongly enhanced due to phonon van Hove singularities. By tuning Δ via gate voltages, one can either control dephasing, or strongly increase emission into phonon modes with characteristic angular distributions.

PACS numbers: 73.21.La, 71.38.-k, 62.25.+g

Coupled semiconductor quantum dots are candidates for controlling quantum superposition and entanglement of electron states. The feasibility of such ‘qubits’ depends on the control of dephasing due to the coupling to low-energy bosonic excitations of the environment. For example, the electronic transport through double quantum dots is determined by the spontaneous emission of phonons even at very low temperatures¹. If two dots are coupled to each other and to external leads, Coulomb blockade guarantees that only one electron at a time can tunnel between the dots and the leads. Dephasing in such a ‘pseudo spin’-boson system^{2,3} is dominated by the properties of the phonon environment.

As a logical step towards the control of dephasing, the control of vibrational properties of quantum dot qubits has been suggested¹. Recently, considerable progress has been made in the fabrication of nano-structures that are only partly suspended or even free-standing^{4,5}. They considerably differ in their mechanical properties from bulk material. For example, phonon modes are split into subbands, and quantization effects become important for the thermal conductivity^{6,7,8}. The observation of coherent phonons in dots⁹ in nanotubes¹⁰ are other examples of low dimensional mesoscopic systems where phonons become experimentally controllable and are the objects of interest themselves.

Double quantum dots are not only tunable phonon emitters¹ but also sensitive high-frequency noise detectors¹¹. Together with their successful fabrication within partly free-standing nanostructures¹², this suggests that they can be used to control both electrons and phonons on a microscopic scale. This opens a path for realizing mechanical counterparts of several quantum optical phenomena, as for instance the generation of non-classical squeezed phonon states¹³ by time-dependent or non-linear interactions with the electrons.

In this paper, we demonstrate that phonon confinement can be used to gain control of dissipation in double quantum dots, leading to a considerable reduction of phonon-induced decoherence. More precisely, we show that inelastic scattering and the inelastic current channel for electron transport in the Coulomb blockade regime

can be drastically reduced as compared to a bulk environment when double dots are hosted by a semiconductor slab that acts as a phonon cavity. This suppression occurs at specific phonon energies $\hbar\omega_0$ when the level splitting is tuned to $\Delta = \hbar\omega_0$. Furthermore, for larger energy differences ε between the two dot ground states, typical properties¹⁴ of a nano-size slab such as phonon-subband quantization can be detected in the staircase-like electronic current $I(\varepsilon)$ through the dots. In addition, and very strikingly, for certain wave vectors we find negative phonon group velocities and phonon van Hove singularities close to which one can strongly excite characteristic phonon modes with specific emission patterns.

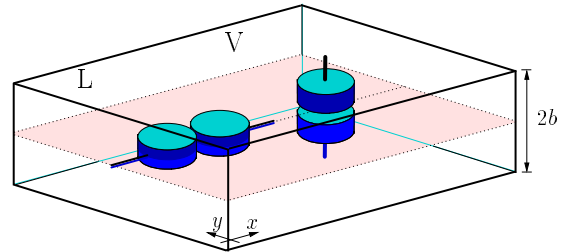


FIG. 1: Scheme for *lateral* (L) and *vertical* (V) configurations of a double quantum dot in a phonon nano-cavity.

The controlled enhancement or reduction of spontaneous light emission from atoms is well-known in cavity QED¹⁵. Here a single, confined photon mode can be tuned on or off resonance with an atomic transition frequency. In contrast to cavity QED, the vanishing of spontaneous emission in phonon cavities is due to real zeros in the *phonon deformation potential or polarization fields* rather than gaps in the density of states. This is a peculiar consequence of the boundary conditions for vibration modes which lead to complicated nonlinear dispersions even for homogeneous slabs. As a result, phonon cavities confined in only one spatial direction support a continuous spectrum, and yet suppression of spontaneous emission is possible.

As a model, we consider two tunnel-coupled quantum dots embedded in an infinite semiconductor slab of thick-

ness $2b$ in a vertical or a lateral configuration, Fig. 1. The dots are weakly coupled to external leads, and we assume that both the energy difference ε and the coupling strength T_c between the dots can be externally tuned by gate voltages. In the Coulomb blockade regime, we adopt the usual description in terms of three many body ground states^{3,16} $|0\rangle$, $|L\rangle$, and $|R\rangle$ that have no or one additional electron in either of the dots, respectively. The coupling to the phonon environment of the slab is described by an effective spin-boson Hamiltonian

$$H = \frac{\varepsilon}{2}\sigma_z + T_c\sigma_x + \sum_{\mathbf{q}} \hbar\omega_{\mathbf{q}}a_{\mathbf{q}}^\dagger a_{\mathbf{q}} + \sum_{\mathbf{q}} (\alpha_{\mathbf{q}}n_L + \beta_{\mathbf{q}}n_R) (a_{\mathbf{q}} + a_{-\mathbf{q}}^\dagger), \quad (1)$$

with $\sigma_z = |L\rangle\langle L| - |R\rangle\langle R|$, $\sigma_x = |L\rangle\langle R| + |R\rangle\langle L|$, $n_i = |i\rangle\langle i|$ and $\alpha_{\mathbf{q}}(\beta_{\mathbf{q}})$ the coupling matrix element between electrons in dot $L(R)$ and phonons with dispersion $\omega_{\mathbf{q}}$.

The stationary current can be calculated by using a master equation³ and considering T_c as a perturbation. We consider weak electron-phonon coupling and calculate the inelastic scattering rate

$$\gamma(\omega) = 2\pi \sum_{\mathbf{q}} T_c^2 \frac{|\alpha_{\mathbf{q}} - \beta_{\mathbf{q}}|^2}{\hbar^2\omega^2} \delta(\omega - \omega_{\mathbf{q}}). \quad (2)$$

For $\hbar\omega = (\varepsilon^2 + 4T_c^2)^{1/2}$ this is the rate for spontaneous emission at zero temperature due to electron transitions from the upper to the lower hybridized dot level.

On the other hand, in lowest order in T_c , the total current $I(\varepsilon)$ can be decomposed into an elastic Breit-Wigner type resonance and an inelastic component $I_{\text{in}}(\varepsilon) \approx -e\gamma(\varepsilon)$, where $-e$ is the electron charge. The double dot, supporting an inelastic current $I_{\text{in}}(\varepsilon)$, therefore can be regarded as an analyzer of the phonon system¹. One can also consider the double dot as an emitter of phonons of energy $\hbar\omega$ at a tunable rate $\gamma(\omega)$. We show below how the phonon confinement within the slab leads to steps in $I_{\text{in}}(\varepsilon)$ and tunable strong enhancement or nearly complete suppression of the electron-phonon coupling.

We describe phonons by a displacement field $\mathbf{u}(\mathbf{r})$ which is determined by the vibrational modes of the slab¹⁷. For the following, it is sufficient to consider dilatational and flexural modes (Lamb waves). The symmetries of their displacement fields differ with respect to the slab's mid-plane. They either yield a symmetric elongation and compression (dilatational mode, Fig. 2 left) or a periodic bending associated with an antisymmetric field (flexural mode, Fig. 2 center). The confinement leads to phonon quantization into subbands. For each in-plane component \mathbf{q}_{\parallel} of the wave vector there are infinitely many subbands, denoted by n , related to a discrete set of transversal wavevectors in the direction of the confinement. Since there are two velocities of sound in the elastic medium associated with longitudinal and transversal wave propagation, c_l and c_t , there are also two transversal wavevectors q_l and q_t . This is in contrast to the isotropic bulk where one can separate the

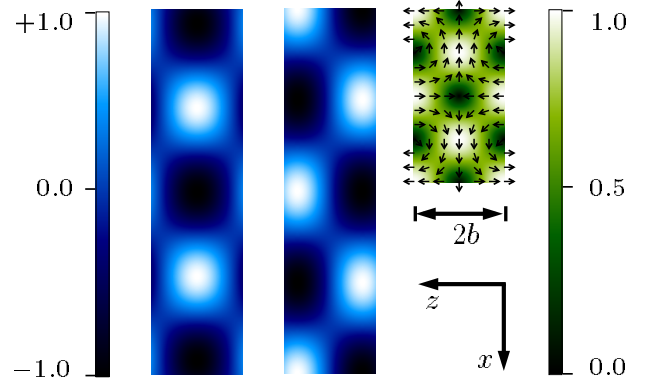


FIG. 2: Deformation potential induced by dilatational (left) and flexural modes (center) at $q_{\parallel}b = \pi/2$ ($n = 2$ subbands). Right: displacement field $\mathbf{u}(x, z)$ of $n = 0$ dilatational mode at $\Delta = \hbar\omega_0$. Greyscale: moduli of deformation potentials (left) and displacement fields (right) (arb. units).

polarizations. For a slab, the boundary conditions at the surface lead to coupling between longitudinal and transversal propagation¹⁴.

We have numerically determined the solutions $q_{l,n}(q_{\parallel})$ and $q_{t,n}(q_{\parallel})$ of the Rayleigh-Lamb equations that describe the dynamics of the confined phonons,

$$\frac{\tan q_{t,n}b}{\tan q_{l,n}b} = - \left[\frac{4q_{\parallel}^2 q_{l,n} q_{t,n}}{(q_{\parallel}^2 - q_{t,n}^2)^2} \right]^{\pm 1} \\ \omega_{n,q_{\parallel}}^2 = c_l^2(q_{\parallel}^2 + q_{l,n}^2) = c_t^2(q_{\parallel}^2 + q_{t,n}^2), \quad (3)$$

together with the dispersion relations $\omega_{n,q_{\parallel}}$ and the displacement field¹⁸ associated with a confined phonon in mode $(n, \mathbf{q}_{\parallel})$. The exponents ± 1 correspond to dilatational and flexural modes, respectively.

The contribution γ_n of subband n to the rate (2) is

$$\gamma_n(\omega) = \sum_{\mathbf{q}_{\parallel}} \frac{|\lambda_{\text{dp/pz}}^{\pm}(\mathbf{q}_{\parallel}, n)|^2}{\hbar^2\omega^2} |\alpha \pm e^{i\mathbf{q}_{\parallel}\mathbf{d}}|^2 \delta(\omega - \omega_{n,q_{\parallel}}) \quad (4)$$

where the vector \mathbf{d} connects the dots and λ is the coupling strength of the electron-phonon interaction. We assume that the electron density is sharply peaked near the dot centers and that the dots are located symmetrically within the slab. We consider both the deformation potential (DP), $\alpha = -1$ in (4), and piezo-electric (PZ) interaction, $\alpha = +1$. The coupling strength for DP is

$$\lambda_{\text{dp}}^{\pm}(q_{\parallel}, n) = B_n^{\text{dp}}(q_{\parallel})(q_{t,n}^2 - q_{\parallel}^2)(q_{l,n}^2 + q_{\parallel}^2) \text{tsc } q_{t,n}b, \quad (5)$$

where $B_n^{\text{dp}} = F_n(\hbar\Xi^2/2\rho\omega_{n,q_{\parallel}}A)^{1/2}$, $\text{tsc } x = \sin x$ or $\cos x$ for dilatational and flexural modes, respectively, Ξ is the DP constant, ρ the mass density, A the area of the slab, and F_n normalizes the n^{th} eigenmode.

First, we discuss the deformation potential interaction in the vertical configuration (Fig. 1), $\mathbf{q}_{\parallel}\mathbf{d} = 0$, where only flexural modes couple to the electrons, whereas dilatational modes lead to a symmetrical deformation field (Fig. 2 left) and yield the same energy shift in both of the dots which does not affect the electron tunneling.

Figure 3 (top) shows $\gamma_{\text{dp}}(\omega)$ in units of the nominal scattering rate $\gamma_0 \equiv T_c^2 \Xi^2 / \hbar \rho c_l^4 b$ for $b = 5d$. The phonon subband quantization appears as a staircase in $\gamma_{\text{dp}}(\omega)$, with the steps corresponding to the onsets of new phonon subbands. Most strikingly, a van Hove singularity (arrow) occurs due to *zero phonon group velocity* at that frequency. This corresponds to a minimum in the dispersion relation $\omega_{n,q_{\parallel}}$ for finite q_{\parallel} with preceding *negative* phonon group velocity due to the complicated non-linear structure of the Rayleigh-Lamb equations for the planar cavity. Additional van Hove singularities occur at higher frequencies (not shown here) as an irregular sequence that can be considered as ‘fingerprints’ of the phonon-confinement in a mechanical nanostructure.

In the lateral configuration (Fig. 1), DP couples only to dilatational modes, in contrast to the vertical case. This is a trivial consequence of the symmetry of the DP of flexural modes (Fig. 2 center) and the fact that in the lateral configuration the dots are aligned mid-plane. The inelastic rate including the lowest 4 modes is shown in Fig. 3 (bottom) in comparison to the bulk rate. The phonon-subband quantization appears as cusps in $\gamma_{\text{dp}}(\omega)$ for $\omega \gtrsim 2\omega_b$. Again, we observe van Hove singularities as fingerprints of the phonon confinement.

Most strikingly, we find a suppression of the inelastic rate at small energies $\hbar\omega$, and even its *complete vanishing* at the energy $\hbar\omega_0 \approx 1.3\hbar\omega_b$ for the lateral configuration. As can be seen from (4) and (5), the rate γ_0 vanishes for the frequency ω_0 defined by the condition $q_t = q_{\parallel}$. This is due to a vanishing divergence of the displacement field \mathbf{u} (Fig. 2 right) that implies vanishing of $\text{DP} \propto \nabla \cdot \mathbf{u}$. Near ω_0 , the remaining contribution of the $n = 0$ -subband mode is drastically suppressed compared with 3d phonons (Fig. 3 bottom, inset).

We checked that this decoupling of electrons and phonons is a generic feature due to the slab geometry, as are the steps and van Hove singularities in γ . For the piezo-electric interaction, our results also reveal a complete vanishing of the inelastic rate γ_{pz} from dilatational phonons at the energy $\hbar\omega'_0 \approx 0.7\hbar\omega_b$ where the induced *polarization field* is zero¹⁹. Due to the symmetry of the latter, in the vertical and lateral configurations only dilatational and flexural phonons, respectively, couple to the electrons via PZ interaction. Thus, the angular dependence is reversed as compared to the DP case.

An important consequence of these results is that one can ‘switch off’ either PZ scattering in the vertical configuration, or DP scattering in the lateral configuration at a certain energy. Then, the only remaining electron-phonon scattering is mediated by the other interaction mechanism that couples the electrons to the flexural modes. For other frequencies ω , the ratio $\gamma_{\text{pz}}/\gamma_{\text{dp}} \propto b^2$

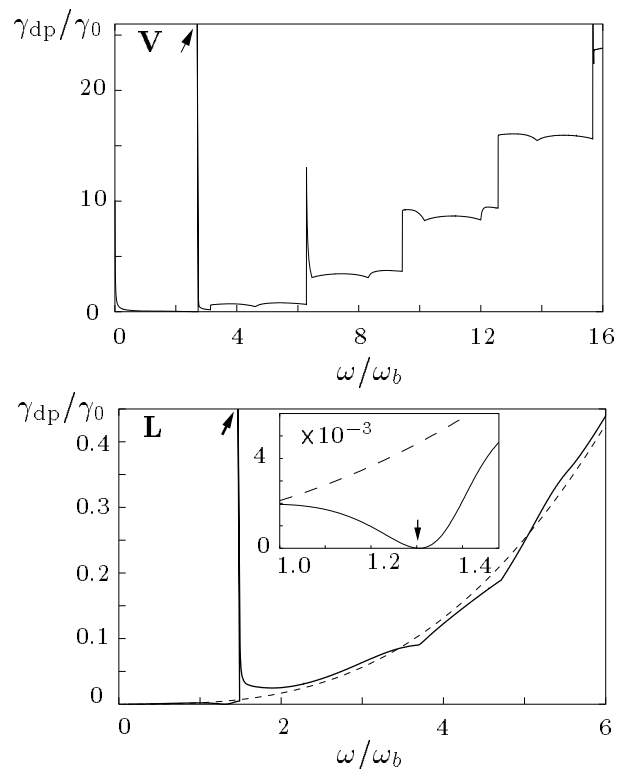


FIG. 3: Inelastic phonon emission rate $\gamma_{\text{dp}}(\omega)$ of vertical (V) and lateral (L) double dots in a phonon cavity of width $2b$ due to deformation potential. Phonon-subband quantization effects appear on an energy scale $\hbar\omega_b = \hbar c_l/b$ with the longitudinal speed of sound c_l ; γ_0 nominal scattering rate (see text). Coupling to *flexural* (top) and *dilatational* modes (bottom, dashed: bulk rate). Inset: Suppression of $\gamma_{\text{dp}}(\omega)$ from slab phonons at $\omega = \omega_0$ (arrow).

can be varied by changing the slab width. Thus, for very small b the DP interaction dominates and the proper choice to ‘switch off’ the scattering would be the lateral configuration, with a small contribution remaining if the material is piezo-electric, and vice versa. For a GaAs slab of width $2b = 1\mu\text{m}$ and a tunnel coupling $T_c = 10\mu\text{eV}$ in the lateral configuration tuned to $\hbar\omega \approx 0.7\hbar\omega_b$ (no PZ coupling), we obtain a residual scattering rate of $\gamma_{\text{dp}} = 8 \cdot 10^4 \text{ s}^{-1}$ from DP-coupling to flexural modes.

The characteristic energy scale for phonon quantum size effects is $\hbar\omega_b \equiv \hbar c_l/b$. Using the same parameters as above, we have $\hbar\omega_b = 7.5\mu\text{eV}$ in GaAs which is within the limit of energy resolution of recent transport experiments in double dots¹. A finite slab of lateral dimension L will lead to a broadening of the structures predicted above since the phonons will acquire a life time $\propto L/c_{l,t}$ which leads to a smearing of fine structures in $\gamma(\omega)$ on an energy scale $\hbar c_{l,t}/L \sim 1\mu\text{eV}$ for $L = 10b$. Finite temperatures yield a similar broadening on a scale $k_B T$. Therefore, low temperatures ($20 \text{ mK} \approx 2\mu\text{eV}$) are required to resolve the step-like features and the van Hove singularities

in the inelastic current I_{in} . We mention that vertically polarized shear waves (which are also eigenmodes of the slab) do not couple to electrons via the DP because the induced local change in volume ($\propto \nabla \cdot \mathbf{u}$) is zero. Fortunately, shear waves also do not change the low frequency decoupling discussed above because the only mode that is accessible at low enough energies is the massless mode (linear dispersion) that does not lead to any piezo-electric polarization field. However, at higher frequencies shear subbands can contribute to the electron scattering.

The existence of an energy $\hbar\omega_0$ where the electron-phonon interaction vanishes could be used to suppress decoherence in double dot qubit systems with the energy difference $\Delta = \sqrt{\varepsilon^2 + 4T_c^2}$ tuned to $\Delta = \hbar\omega_0$. For example, using gate voltages to tune $T_c(t) = \Delta/2 \sin(\Omega t)$, $\varepsilon(t) = \Delta \cos(\Omega t)$ as a function of time defines a one-qubit rotation ('electron from left to right') free of phonon interaction $\propto \gamma(\Delta) = 0$. The condition $\Delta = \hbar\omega_0$ therefore defines a one dimensional 'dissipation-free manifold' (curve) in the T_c - ε parameter space. In particular, a suppression of decoherence could then be exploited in adiabatic electron transfers²⁰ or adiabatic swapping operations²¹ in coupled quantum dots.

We recall, however, that corrections to γ of 4th and higher order in the coupling constant (virtual processes) can lead to a small but final phonon-induced dephasing rate even at $\Delta = \hbar\omega_0$. Moreover, the dephasing due to spontaneous emission of photons, although negligible with respect to the phonon contribution in second order¹, is not altered unless the whole system is embedded into a photon cavity. Similarly, plasmons and electron-hole pair excitations in the leads can lead to dephasing. We suppose that the latter can affect the inter-dot dynamics of the coupled dots only indirectly via coupling to the leads and only weakly contribute to dephasing, as is

the case for interactions between dot and lead electrons beyond the Coulomb blockade charging effect.

Alternatively to suppressing dissipation from phonons at certain energies, the van Hove singularities of the same system could be used to enormously enhance the spontaneous emission rate of phonons. The electron current $I_{\text{in}} \approx -e\gamma(\varepsilon)$ at those energies is due to strong inelastic transitions. The term $|\alpha \pm e^{i\mathbf{q}\cdot\mathbf{d}}|^2$ in (4) determines the angular phonon emission characteristic of the double dot. Therefore, as a function of energy and orientation, the double dot can be used as an energy selective phonon emitter with well defined emission characteristics.

In conclusion, we have found that phonon confinement is a promising tool for gaining control of dephasing in double quantum dots via phonons. Once this was achieved, it would be possible to study systematically dephasing due to other mechanisms such as coupling to electronic excitations in the leads. In contrast to cavity QED, where a single, confined photon mode can be tuned on or off resonance with an atomic transition frequency, the vanishing of spontaneous emission in phonon cavities is due to zeros in the *phonon deformation potential or polarization fields* rather than gaps in the density of states. In addition, we found that phonon emission into characteristic modes can be enormously enhanced due to van Hove singularities that could act as strong fingerprints of the phonon confinement if experimentally detected.

This work was supported by the EU via TMR and RTN projects FMRX-CT98-0180 and HPRN-CT2000-0144, DFG projects Kr 627/9-1, Br 1528/4-1, and project EPSRC R44690/01. Discussions with R. H. Blick, T. Fujisawa, W. G. van der Wiel, and L. P. Kouwenhoven are acknowledged.

-
- ¹ T. Fujisawa *et al.*, Science **282**, 932 (1998); S. Tarucha *et al.*, Microelectr. Engineer. **47**, 101 (1999).
² A. J. Leggett *et al.*, Rev. Mod. Phys. **59**, 1 (1987).
³ T. Brandes and B. Kramer, Phys. Rev. Lett. **83**, 3021 (1999).
⁴ A. N. Cleland and M. L. Roukes, Nature **392**, 160 (1998).
⁵ R. H. Blick *et al.*, Physica B **249**, 784 (1998).
⁶ J. Seyler and M. N. Wybourne, Phys. Rev. Lett. **69**, 1427 (1992).
⁷ A. Greiner, L. Reggiani, T. Kuhn, and L. Varani, Phys. Rev. Lett. **78**, 1114 (1997).
⁸ L. G. C. Rego and G. Kirczenow, Phys. Rev. Lett. **81**, 232 (1998).
⁹ T. D. Krauss and F. W. Wise, Phys. Rev. Lett. **79**, 5102 (1998).
¹⁰ M. S. Dresselhaus and P. C. Eklund, Adv. Phys. **49**, 705 (2000).
¹¹ R. Aguado and L. Kouwenhoven, Phys. Rev. Lett. **84**, 1986 (2000).
¹² R. H. Blick *et al.*, Phys. Rev. B **62**, 17103 (2000).
¹³ X. Hu and F. Nori, Phys. Rev. Lett. **79**, 4605 (1997).
¹⁴ T. Meeker, and A. Meitzler, in *Physical Acoustics* (Academic, New York 1964), Vol. 1, Part A; B. Auld, *Acoustic Fields and Waves* (Wiley, New York 1973), Vol. 2.
¹⁵ G. S. Argawal, *Fundamentals of Cavity Quantum Electrodynamics* (World Scientific, Singapore 1994).
¹⁶ T. H. Stoof and Yu. V. Nazarov, Phys. Rev. B **53**, 1050 (1996).
¹⁷ L. D. Landau and E. M. Lifschitz, *Course of Theoretical Physics* (Butterworth-Heinemann, Oxford 1986), Vol. 7.
¹⁸ N. Bannov *et al.*, Phys. Rev. B **51**, 9930 (1995); N. Bannov *et al.*, phys. stat. sol. (b) **183**, 131 (1994).
¹⁹ S. Debal, T. Brandes, and B. Kramer, unpublished.
²⁰ F. Renzoni and T. Brandes, Phys. Rev. B **64**, 245301 (2001).
²¹ J. Schliemann, D. Loss, and A. H. MacDonald, Phys. Rev. B **63**, 085311 (2001).